Noise Generation by Porous Airfoils

Ennes Sarradj* and Thomas Geyer†
Institute of Traffic Research, BTU Cottbus, 03046 Cottbus, Germany

The noise generated by the flow around airfoils continues to be one of the important aeroacoustic noise sources. Innovative techniques for airfoil noise reduction are, therefore, of great importance. The present experimental study deals with the use of porous material for the construction of airfoils and the subsequent noise reduction. The use of such material controls the flow around the airfoil and has an influence on the sound generation. The analysis focuses on the characterization of the influence of the porous material parameters, especially the flow resistivity and the porosity, on the noise generation. Results of aeroacoustic wind tunnel tests on several porous and non-porous SD 7003 model scale airfoils are compared. Using microphone array measurements, it was found that not only the overall sound pressure level, but also the spectral characteristics depend on the parameters of the porous material. While the overall sound pressure level decreases in the order of a few decibel, at lower frequencies the reduction is considerable larger and extends 10 dB in some cases. Additionally, the influence of the material parameters on drag and lift is discussed. The aerodynamic performance of the porous airfoils is in general inferior to that of non-porous airfoils. However, there appear to be sets of material parameters that provide a considerable decrease in sound generation and only a minor degradation of aerodynamic effciency.

Nomenclature

$\mathbf{e}$	Steering vector
$\mathbf{S}$	Cross spectral matrix
$\mathbf{W}$	Weight matrix
p	Sound pressure
D	Drag force
L	Lift force
L	Sound pressure level
P	Pitch moment
S	Side force
S	Power spectrum
R	Roll moment
U	Airflow speed
Y	Yaw moment
Δx	Sample thickness
ρ	Mass density
σ	Porosity
ω	Angular frequency
Ξ	Flow resisitivity

*Junior Professor, Institute of Traffic Research, BTU Cottbus, Siemens-Halske-Ring 14, 03046 Cottbus, Germany.
†Research Assistant, Institute of Traffic Research, BTU Cottbus, Siemens-Halske-Ring 14, 03046 Cottbus, Germany.

I. Introduction

A scenario quite often encountered in aeroacoustic noise control is the noise generated by the flow around a solid body. A number of approaches have been developed in the past to tackle the problem of reducing this noise, including techniques to find aeroacoustic favorable shapes for such bodies. Another approach is to alter the material the body is made of. In most engineering constructions the bodies which might placed in flow such as strut- and rod-like parts exposing from the hull of high speed vehicles, ventilator blades, grids, airfoils and so on are made of rigid material. If this material is replaced by a porous material, a reduction of the noise generated may be observed. In this context the term porous material is applied to materials that have open and interconnected pores, so that air flow may enter them. This applies for instance to certain types of synthetic or metallic foams.

The approach of porous material application for flow noise reduction was subject to a number of studies in the past. Hayden et. al.[1] propose foil structures with reduced sound generation, claiming a considerable reduction of sound power levels for a model scale airfoil. Some experimental studies conclude that fan noise can be reduced by the application of porous material blades.[2,3] Experiments on a model scale wing of a Lockheed L 1011 with flaps with porous surfaces have shown a noise reduction between 0 und 2 dB,[4] depending on the parameters of the porous material used. For the reduction of rotor and turbomachinery noise the use of porous material has been considered for the vane leading edge.[5] More recently, a number of numerical studies have focused on the application of porous material for slat trailing edges,[6] on rotor tips,[7] as well as on turbofan stator vanes.[8] While it is agreed that the application of porous materials may have an important potential for flow noise reduction,[9,10] it is also stated that it is necessary to develop more comprehensive models for the influence of porous material parameters.

The aim of the present study is to go one step into that direction. Despite the number of studies in the past there seems to be no agreement about the mode of operation of the porous material or the porous treatments. If we restrict ourselves to the very generic example of the noise generated by an airfoil in flow, then a number of candidate mechanisms come into view, that might reduce the sound generation. The first of these mechanisms is acoustic absorption. It is well known that porous materials may be applied to absorb acoustic energy by the viscous and thermal losses that occur during the oscillatory fluid motion in the pores of a porous material. However, in the usual application of such porous sound absorbers, for an effective sound reduction the absorber requires to be not small compared to the acoustic wavelength, as this was the case in at least some of the experiments mentioned above. Another possible mechanism is the dissipation of turbulent energy from the boundary layer by the porous surface. This would also result in less broadband noise generation at the trailing edge. A third mechanism could be the correspondence of the lower and the upper boundary layer through the porosity of the airfoil. Especially in the aft part of the airfoil this will reduce the dynamic pressure differences at the trailing edge and therefore also the trailing edge noise in the same fashion as a serrated trailing edge works[11] for reduced sound generation. Additionally, porosity may have an reducing influence on noise generated by the contact of turbulence with the leading edge and also on other noise generating mechanisms. Regardless of what mechanism is responsible it is obvious that the porous material properties should have an influence on the sound reduction.

To characterize this influence somewhat further, the present experimental study compares the sound generation by different porous airfoils and one non-porous airfoil, all having the same size and shape. Additionally, the aerodynamic behavior was compared by measuring lift and drag.

II. Airfoil Models

The aeroacoustic and aerodynamic tests were conducted on six airfoil models. For all airfoils an identical geometry was chosen. This is the SD 7003 type (see fig. 1), a half-symmetric airfoil for low Reynolds numbers invented by Selig and Donovan.[12] Each model has a chord length of 235 mm, a maximum camber of 20 mm and a wingspan of 400 mm.

Up to six physical meaningful parameters can be used to characterize porous materials having a rigid frame. For the purpose of this paper only two of them should be considered. The first parameter is the porosity σ, defined as the ratio of the pore volume V_P to the total volume V_T of a sample of material. To establish a more exact definition, it must be considered that in general the pore volume may consists of such pores that correspond with each other and with the surrounding and of other pores that are closed and isolated. Only the former are expected to have an influence on the acoustical and aerodynamical

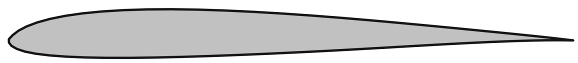

Figure 1. Side view of an SD 7003 airfoil

characteristics, so it is convenient to define an accessible porosity on the basis of the accessible pore volume:

$$\sigma = \frac{V_A}{V_T}. \tag{1}$$

The (total) porosity may be estimated from the mass density of the sample ρ_A and that of the constituents of the frame ρ_F:

$$\sigma = \frac{\rho_A}{\rho_F}. \tag{2}$$

In order to determine the porosity, the samples used were weighted and this relation was applied.

The flow resistance is the second parameter that should be considered here. It is the ratio of the pressure drop Δp across a sample when a static flow of mean velocity U is applied to a sample. The flow resistivity Ξ is the flow resistance normalized with respect to the sample thickness Δx and is a more appropriate measure to characterize the material instead of the sample:

$$\Xi = -\frac{\Delta p}{U \Delta x}. \tag{3}$$

For the measurement of the flow resistance of the samples a computer controlled apparatus was used.

For the manufacturing of test specimen different porous materials have been examined for their potential porosity and flow resistivity, their availability and their quality with respect to different manufacturing technologies. These materials were, amongst others, various synthetic foams, metallic and ceramic foams and felts. The materials chosen for the manufacturing of the five porous airfoils are:

- *Basotect*, a synthetic foam designed for use as porous sound absorber,
- three different types of *Panacell*, again a synthetic foam, with three different pore densities of 45, 60 and 90 pores per inch (ppi),
- *Reapor*, a material made of porous glass pellets.

Table 1 on the following page gives an overview of the acoustic parameters that have been measured on the five porous materials. While the porosity is in all cases very close to 1, the flow resistivity is quite different.

The non-porous airfoil is made of laminated fiber board with a special finish to yield a smooth surface. The porous airfoils have been manufactured using water jet cutting technology. Compared to other technologies like laser-cutting or milling the jet cutting provides the advantage of preventing the open pores of the materials from damage. Furthermore, this method enables the cutting of complex geometries very fast and exact. Figure 2 on the next page shows two of the airfoils used in the tests.

III. Experimental Approach

The experiments were conducted at the aeroacoustic wind tunnel at technical university of Cottbus (BTU). This facility is an open jet wind tunnel especially designed for very quiet flow. With the circular nozzle used for the tests, the jet diameter is 20 cm and the maximum flow speed is 60 m/s. The test room is reverberant, but for the tests reported here a booth equipped with absorbing material was applied to the tunnel outlet. If the tunnel is operated without any test object in the jet, the A-weighted tunnel self noise is only 61 dB at 50 m/s.

The test program for the six airfoils was to measure both the sound emission from the airfoil and the aerodynamic forces acting for six different angles of attack and 15 different wind speeds. A schematic of the test set-up used for the experiments is shown in figure 3 on page 5. The airfoil under test is placed in front

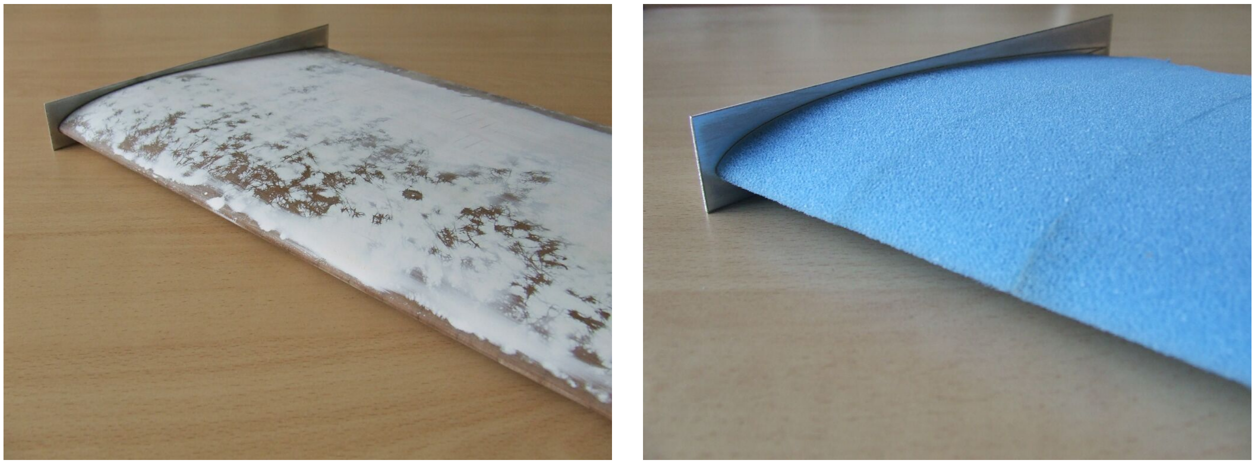

(a) non-porous: laminated fiber board with finish

(b) porous: Panacell 45 ppi

Figure 2. Two of the airfoils used in the tests

Table 1. Flow resistivity and porosity of the porous materials (1 Pas/m^2 = 1 MKS rayls/m)

no.	airfoil material	flow resistivity Ξ Pa s/m^2	porosity σ
1	non-porous	∞	0
2	Basotect	9810	0,997
3	Panacell 45 ppi	730	0,993
4	Panacell 60 ppi	3560	0,991
5	Panacell 90 ppi	4000	0,990
6	Reapor	16500	0,968

of the nozzle. Thus, the laminar core jet as well as the the more turbulent mixing region of the jet have contact with the airfoil. Both regions of flow are of interest because both laminar and turbulent inflow may generate sound at the airfoil.

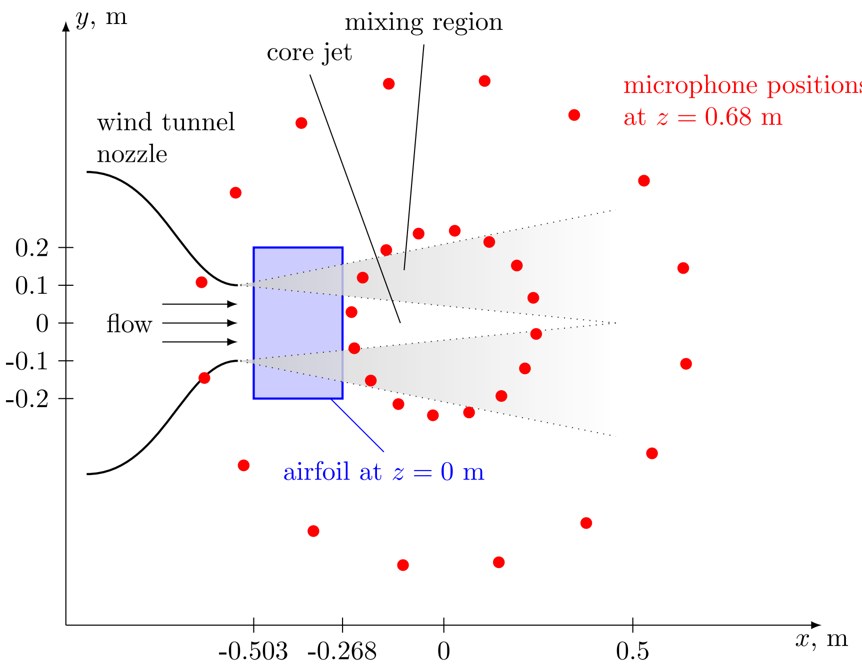

Figure 3. Schematic of the test set-up

The airfoil model is attached to a carrier, which is used to adjust the angle of attack and the position of the airfoil regarding to the nozzle of the wind tunnel. A purposely constructed six-component balance (figure 5 on the next page) on the carrier measures the different forces and moments that occur at the airfoil. These are the lift L, drag D, and side force S and the rolling moment R, the pitching moment P, and the yawing moment Y as can be seen in figure 4. In the present case, with the air flowing in the direction of the x-axis

$$S = 0, \; R = 0, \; Y = 0 \tag{4}$$

are valid because the airfoil is fixed on both sides, and both flow and airfoil are symmetric with respect to the plane $y = 0$. The remaining forces L and D and the pitching moment P of each of the six airfoils have been measured, but only the results for L and D are reported in this paper.

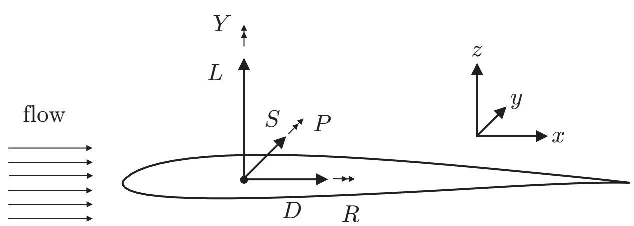

Figure 4. Forces and moments at an airfoil

A microphone array mounted above the airfoil was used for the acoustical measurements. It is placed outside the flow 0.68 m apart from the airfoil and consists of 56 electret microphones flush mounted in a plate (see figure 5 on the next page). In the test, 32 of these microphones layed out in a two circle geometry (see figure 3) were used. In order to obtain a good resolution at low frequencies, the applied array geometry has a large diameter of approximately 1.30 m. The two circle geometry is optimized to maintain a satisfactory side-lobe suppression at higher frequencies at the same time. The signals from the microphones were fed into a computer using a 32-channel front end with a resolution of 24 bit per channel manufactured by National Instruments and processed using in-house developed software.

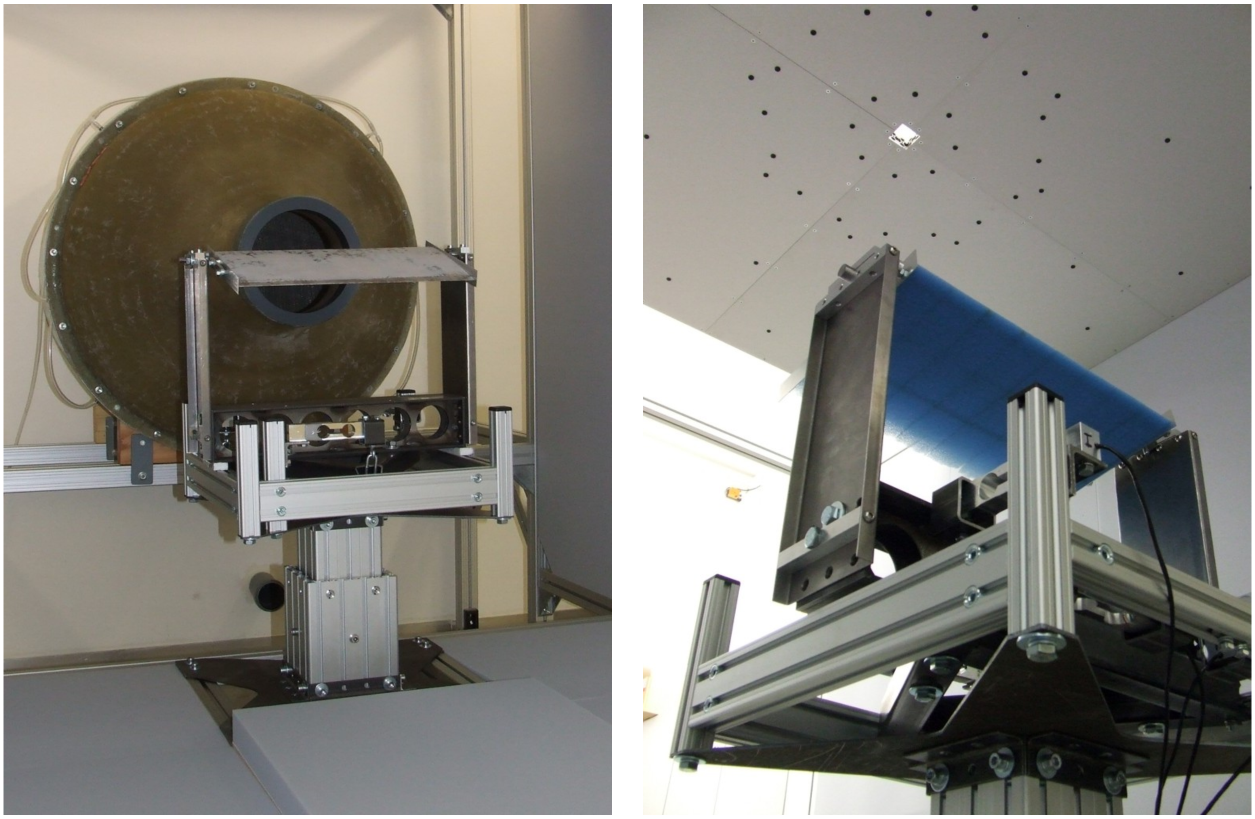

(a) seen from downstream: airfoil, nozzle (behind), balance (below)

(b) seen from below: balance, airfoil, microphone array

Figure 5. Photographs of set-up in wind tunnel

IV. Data Processing

The measurements according to the test program with six angles of attack and 15 different wind speeds for each of six airfoils sum up to a total of 540 single acoustic and aerodynamic measurements. Thus, it was unavoidable to set up an appropriate computer database which allows for easy automated access to all results. While the processing of wind tunnel operation parameters and aerodynamic results is straightforward, the processing of the data from the microphone array requires some comments.

A microphone array is applied in the present case to extract as much information an possible from the measurement. Of particular interest is the sound level generated by different source mechanisms and the source location. Even in the quiet environment of the aeroacoustic wind tunnel there is some unwanted noise that might pollute the measurement. Therefore, the use of the array instead of single microphone shall not only obtain source level and location but also remove the influence of the unwanted noise from the results. As microphone arrays are widely used in aeroacoustic testing, a number of methods for the processing of the microphone signals have been developed. The method applied in the present case bases on the orthogonal beamforming method, a variant of the delay-and-sum beamformer. A brief explanation shall be given here, while more details may be found in another paper.[13] The output power spectrum of a conventional delay-and-sum beamformer is:

$$S(\omega) = \frac{\mathbf{e}(\overrightarrow{x_0})^H \mathbf{W} \mathbf{S}_{\mathbf{xy}} \mathbf{W}^H \mathbf{e}(\overrightarrow{x_0})}{(\operatorname{trace} \mathbf{W})^2}, \tag{5}$$

where $\mathbf{e}(\overrightarrow{x_0})$ is the so called steering vector, that steers the directional characteristic of the beamformer to $\overrightarrow{x_0}$,

$\mathbf{W}$ is a diagonal matrix where w_i weighting factors populate the main diagonal and $\mathbf{S_{xy}}$ is an estimate of the cross spectral matrix of the microphone signals. This spectrum corresponds to the sound level contribution from $\overrightarrow{x_0}$ in the array phase centre location, that equals to $(x, y, z) = (0, 0, 0.68)$ m for the present set-up:

$$L_S(\omega, \overrightarrow{x_0}) = 10 \lg \left(\frac{S(\omega)}{p_0^2} \right) \text{dB}. \tag{6}$$

If the sound field is considered to be a superposition of orthogonal sound fields from a number of uncorrelated sources, it can be shown that the contribution from each of these sources may be computed independently by:

$$S(\omega)_j = \frac{\mathbf{e}(\overrightarrow{x_0})^H \mathbf{W} \left(\mathbf{S_{xy}}_j - \operatorname{diag} \mathbf{S_{xy}}_j \right) \mathbf{W}^H \mathbf{e}(\overrightarrow{x_0})}{(\operatorname{trace} \mathbf{W})^2 - \operatorname{trace} \mathbf{W}}, \tag{7}$$

where $\mathbf{S_{xy}}_j$ is the component from an eigenvector-eigenvalue decomposition of the cross spectral matrix that corresponds to the source j. Also applied in equation (7) is the removal of the main diagonal which has shown to remove unwanted noise.[14]

The orthogonal beamforming technique enables the construction of a map of the sound pressure contribution from each sound source. Then, each of these maps may be examined for the location of the strongest apparent source, which will be the location of the sound source, that is not necessarily a point source. This procedure enables to assign the individual sources and their source strengths respective their sound pressure contributions to source domains. Thus, it is possible to quantitatively assess the sound pressure contribution from a certain area in the map without the need to perform an integration over the sound pressure map. Figure 6 on the next page illustrates the technique using an example from the present test set-up. As the orthogonal beamforming and postprocessing is done one a per frequency basis, it is also possible to estimate quantitative source spectra.

For the acoustical measurements with the microphone array, all the results reported in the following section were computed from the signals sampled during a time window of 1 s at a sampling rate of 48 kHz. The cross spectral matrices for the beamforming algorithm were computed from the average of 747 FFT operations with 256 samples, overlap 75% and von-Hann windows applied.

V. Results

While a large amount of data was acquired and analyzed in the experiments, only a fraction of it can be presented in this paper. Because many of the results at different wind speeds show quite similar behavior, the results presented here are shown for the maximum wind speed of 50.2 m/s unless otherwise noticed.

Airfoils made of porous material have a more or less rough surface. Thus, it can be expected that the drag force acting on an porous airfoil is much higher as that for a smooth-surfaced non-porous airfoil. For similar reasons, especially for the possible flow through the porous airfoil it can be also expected to have a smaller lift. Figure 7 on page 9 shows the results of the aerodynamic measurements that agree with that expectation. Moreover, it can be concluded that both the drag and the lift depend on the flow resistivity Ξ of the material (see also table 1 on page 4). The higher the flow resistivity is, the higher is also lift. The Reapor airfoil with the highest flow resistivity of the materials under test has also the highest lift of all porous airfoils and is not much inferior to the non-porous airfoil. The airfoil made of Panacell 45 ppm with the lowest flow resistivity has the smallest lift and also the highest drag. It may concluded that in general the aerodynamic performance is governed by the flow resistivity. Those airfoils made of porous material with high flow resistivity have a higher lift and lower drag.

Depending on the different possible mechanisms for noise generation, different possible source domains were analyzed during the processing of the measured data from the array. In detail, these domains are: the domain of the whole airfoil with a 5 cm margin around it, the domain of the trailing edge with a similar margin, and the domain of airfoil within the core of the free jet. The domains are depicted in figure 8 on page 10. As can be seen, the whole airfoil domain overlaps the trailing edge and the core jet domain. Therefore, the sources from the latter two are also included in the former source domain. Figure 9 on page 10 shows the spectra from the sources in the whole airfoil domain for different angles of attack. Interestingly enough, the non-porous airfoil produces the highest level in nearly all cases and has a spectrum that decreases monotonously toward higher frequencies with a nearly constant slope. On the other hand side, the spectra

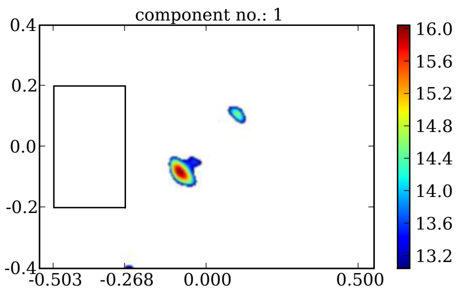

(a) (rejected)

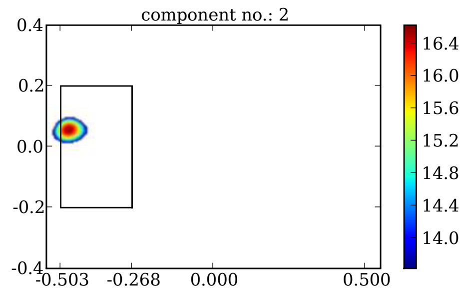

(b) (accepted)

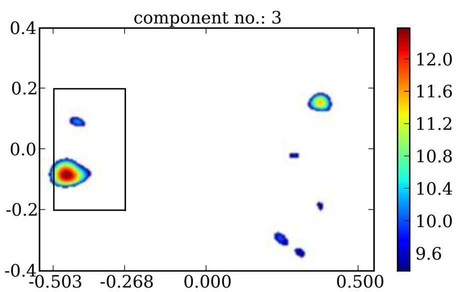

(c) (accepted)

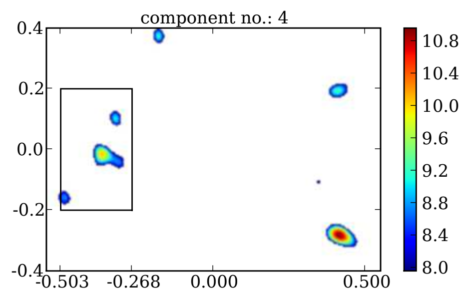

(d) (rejected)

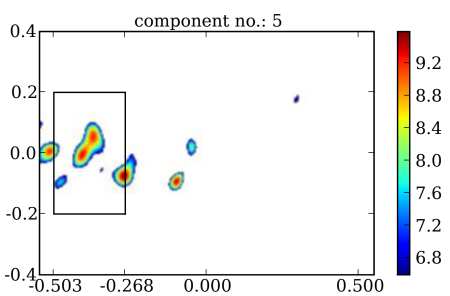

(e) (accepted)

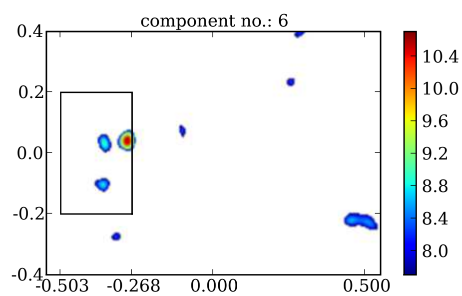

(f) (accepted)

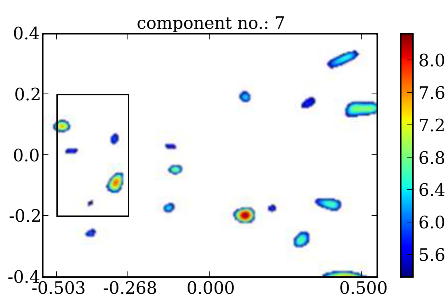

(g) (rejected)

Figure 6. Example for the technique to assign individual sources to source domains: a wind tunnel measurement on a porous Basotect airfoil (shown as black outlined rectangle) at 22.3 m/s and 0° angle of attack. The maps of sound pressure show the contributions at 4 kHz from first seven components from orthogonal beamforming. If the strongest apparent source is in the rectangle, then this is a source from airfoil (=accepted), if not, then it is unwanted background noise (=rejected). Note the extremely low sound pressure levels. The dynamic range of the maps is set to only 3 dB for the sake of clarity.

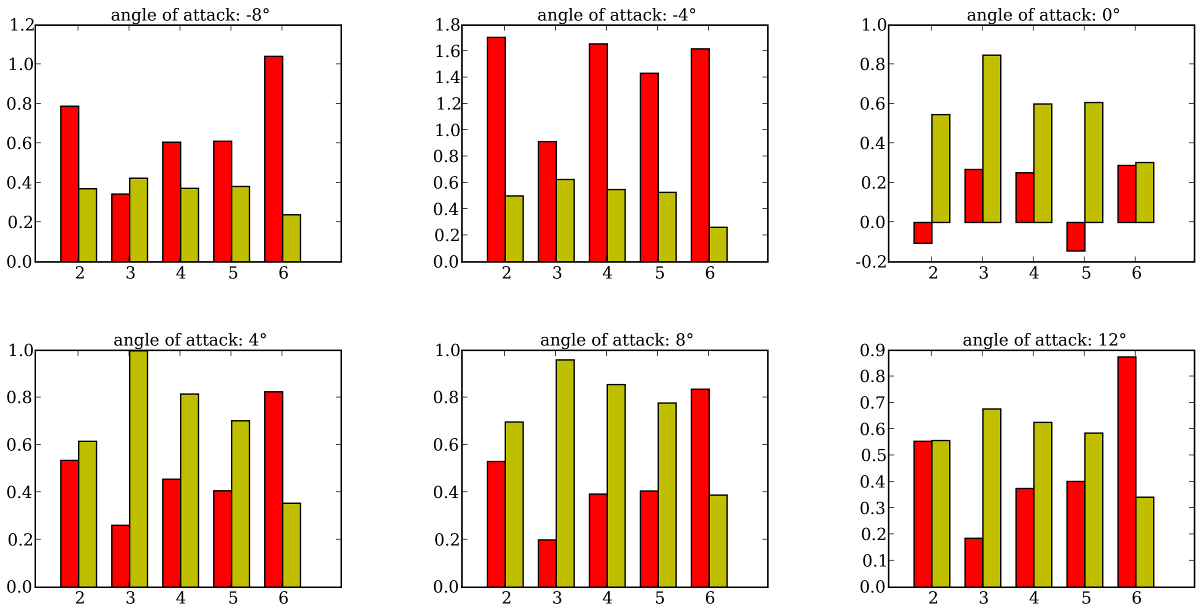

Figure 7. Results of aerodynamic measurements: lift and drag of the porous airfoils normalized to that of the non-porous airfoil. Note that the reading for drag must be multiplied by a factor of 10 to get the correct result. For angles of attack $< 0^\circ$, the lift of both porous and non-porous airfoils is negative. The numbers on the abscissa correspond to those given in table 1 on page 4.

from the porous airfoils tend to have a slope more gradual at higher Frequencies. This is especially true for the Reapor airfoil with the highest flow resistivity. While the level from this airfoil is generally the lowest for low frequencies, at high frequencies it is even higher than that from the non-porous airfoil. For lower wind speeds, this property can also be observed at the spectra from the other porous airfoils, see figure 10 on the following page. It appears also that the noise spectrum is governed by the properties of the porous material. However, no simple relation between the properties from table 1 on page 4 and the spectrum can be drawn from the present results.

The characteristics of these spectra could indicate that the source mechanism that governs the noise generation for the non-porous airfoil is less important, but another mechanism with another type of spectrum dominates at least for high frequencies. Figures 11 and 13 grant some more insight: the trailing edge noise spectra and even more the core jet domain spectra in figure 11 on page 11 show that the sources for high-frequency noise must be located in the remaining domain, where the mixing region of the jet impinges the airfoil. This can also be seen from the source maps plotted in figure 13 on page 12. For the non-porous airfoil the trailing edge is clearly the most important source for all frequencies. While for 1 and 2 kHz octave bands the trailing edge noise dominates also the noise from the porous airfoil, beginning with the 4 kHz octave band this is no longer true and for 16 kHz the trace of the boundary between core jet and mixing region can clearly be seen on the airfoil, indicating this is a the major source region. However, because the low frequencies dominate the noise, this has no serious effect on the overall sound pressure. Figure 12 on page 11 shows the results for the overall sound pressure level for different angles of attack. From the results a simple conclusion similar to that for the aerodynamic behavior is not possible. The noise reductions for the Basotect and Panacell airfoils are different for each angle of attack. Only the Reapor airfoil appears to be favorable for all configurations.

VI. Conclusion

To analyze the noise generation by airfoils made of porous material, five porous and one non-porous SD 7003 airfoils were tested. A large number of measurements were conducted at different wind speeds and angles of attack. Acoustic as well as aerodynamic measurements were performed.

From the aerodynamic results it can be concluded that lift is increased and drag is decreased with

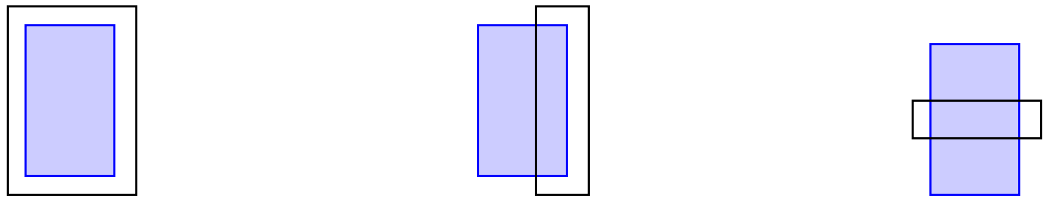

(a) whole airfoil (b) trailing edge (c) core domain

Figure 8. Location of source domains with respect to the airfoil.

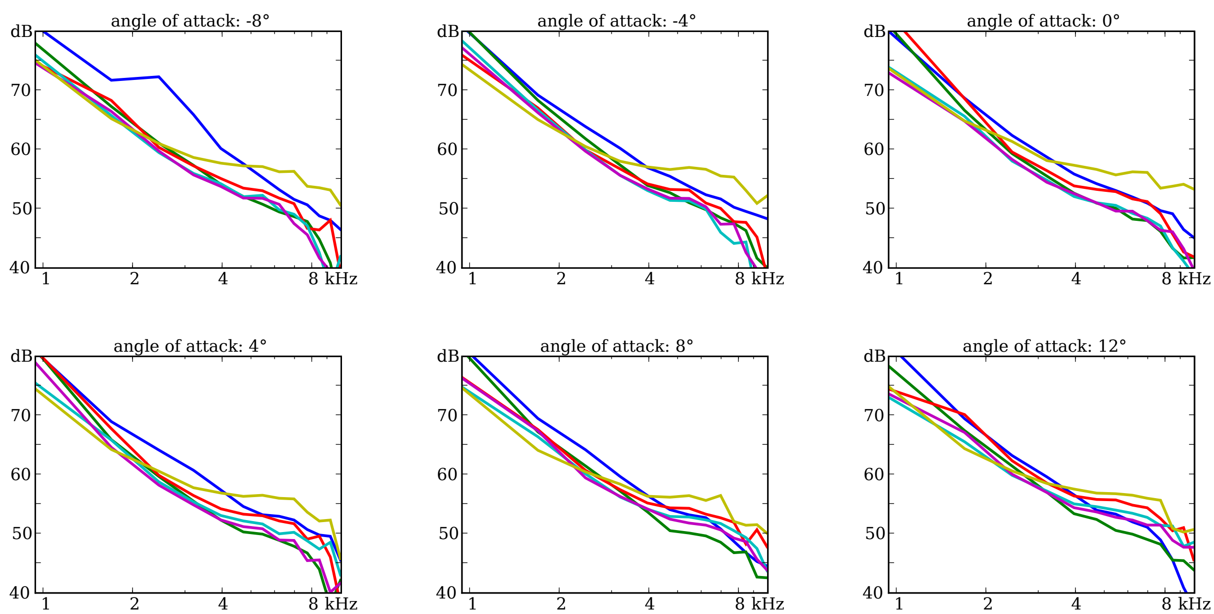

Figure 9. Spectra for the source domain of the whole airfoil for different angles of attack and a wind speed of 50.2 m/s.
non-porous, Basotect, Panacell 45 ppi, Panacell 60 ppi, Panacell 90 ppi, Reapor

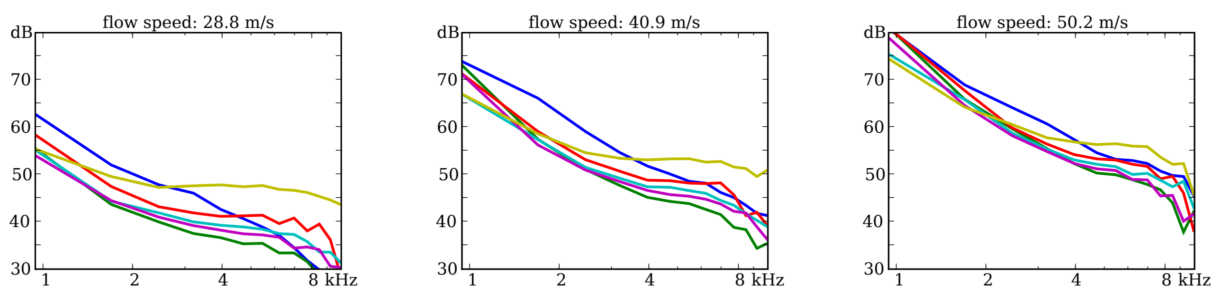

Figure 10. Spectra for the source domain of the whole airfoil for 4° angle of attack and for different wind speeds.
non-porous, Basotect, Panacell 45 ppi, Panacell 60 ppi, Panacell 90 ppi, Reapor

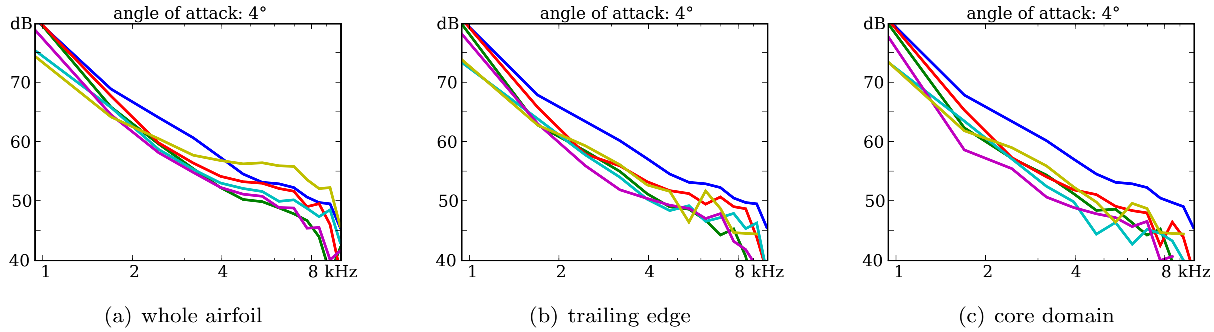

(a) whole airfoil (b) trailing edge (c) core domain

Figure 11. Spectra for different source domains from figure 8 on the preceding page for 4° angle of attack and a wind speed of 50.2 m/s.
—non-porous, —Basotect, —Panacell 45 ppi, —Panacell 60 ppi, —Panacell 90 ppi, —Reapor

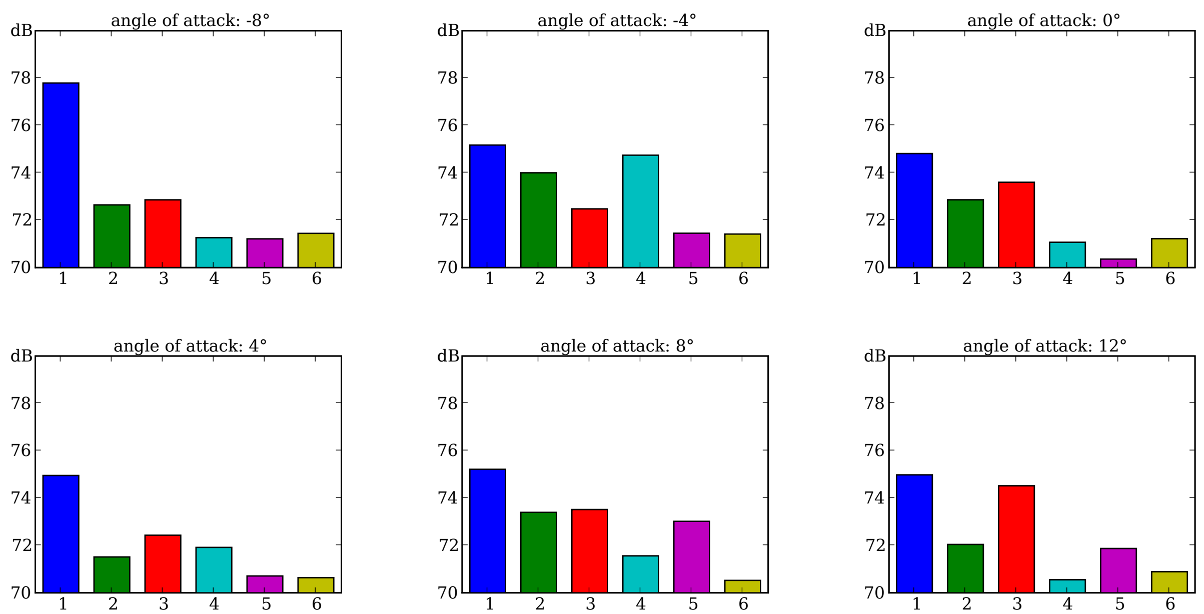

Figure 12. Overall level for the frequency band 750 Hz - 20 kHz, for the source domain of the whole airfoil for different angles of attack and a wind speed of 50.2 m/s.
non-porous, Basotect, Panacell 45 ppi, Panacell 60 ppi, Panacell 90 ppi, Reapor

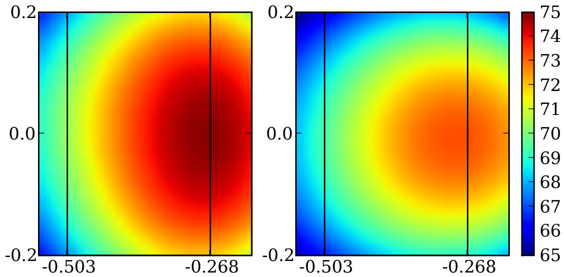

(a) 1 kHz octave band

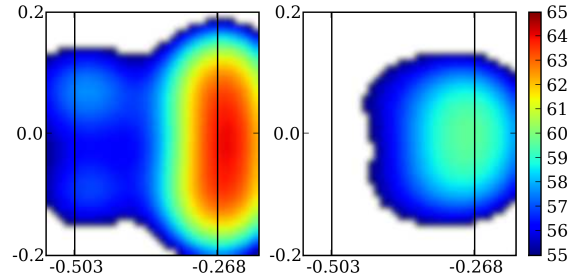

(b) 2 kHz octave band

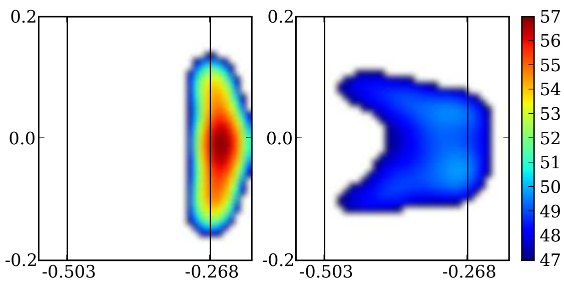

(c) 4 kHz octave band

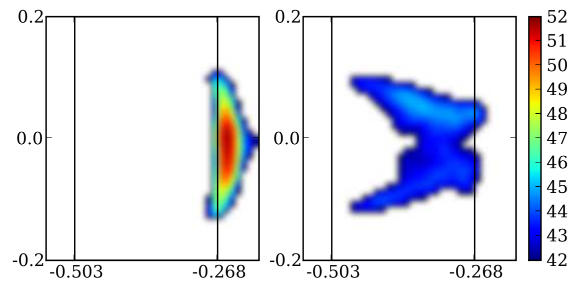

(d) 8 kHz octave band

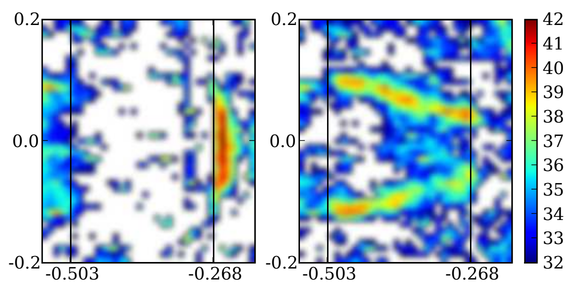

(e) 16 kHz octave bandx

Figure 13. Comparison of source maps for the non-porous airfoil (left) and the Panacell 45 airfoil (right) for for 4° **angle of attack and a wind speed of 50.2 m/s.**

increasing flow resistivity of the porous material of an airfoil. For the acoustic results such simple dependence was not found. For the source mechanisms the results indicated that for both non-porous and porous airfoils trailing edge noise dominates the noise if the airfoil is in a low turbulence flow as this is the case in the core of the wind tunnel free jet. While the contact zone between turbulence from the mixing region and the airfoil is no dominant noise source for the non-porous airfoil, this is the case for the porous airfoils at high frequencies. The intensity of this source mechanism and therefore also the spectrum of the overall noise is controlled by the properties of the porous material, but again no simple relation to the material parameters is obvious. A last conclusion that may be drawn especially from the results for the Reapor airfoil is that there appear to be sets of material parameters that provide a considerable decrease in sound generation and only a minor degradation of aerodynamic effciency.

Acknowledgments

This work was sponsored by the Deutsche Forschungsgemeinschaft under reference number SA 1502/1-1.

References

[1]Hayden, R. and Chanaud, R., "Foil structures with reduced sound generation," Us. Patent 3853428, 1974.

[2]Choroschew, G., Petrow, J., and Jegorow, N., *Schum sudowich sistem*, isdatelstwo sudostrojenije, 1974.

[3]Chanaud, R., Kong, N., and Sitterding, R., "Experiments on porous blades as a means of reducing fan noise," *The Journal of the Acoustical Society of America*, Vol. 59, 1976, pp. 564.

[4]Revell, J., Kuntz, H., Balena, F., Horne, W., Storms, B., and Dougherty, R., "Trailing Edge Flap Noise Reduction by Porous Acoustic Treatment," *3rd AIAA/CEAS Aeroacoustics Conference*, No. AIAA-97-1646-CP, 1997.

[5]Lee, S., *Effect of leading-edge porosity on blade-vortex interaction noise.*, 1993.

[6]Khorrami, M. and Choudari, M., "Application of Passive Porous Treatment to Slat Trailing Edge Noise," Tech. Rep. TM-203-212416, NASA, 2003.

[7]Khorrami, M. and Choudari, M., *A Novel Approach for Reducing Rotor Tip-Clearance Induced Noise in TurbofanEngines*, 2001.

[8]Tinetti, A., Kelly, J., Thomas, R., and Bauer, S., *Reduction of Wake-Stator Interaction Noise Using Passive Porosity*, 2002.

[9]Lockard, D. and Lilley, G., "The Airframe Noise Reduction Challenge," Tech. Rep. TM-2004-213013, NASA, 2004.

[10]Rackl, G., Miller, G., Guo, Y., and Yamamoto, K., "Airframe Noise Studies - Review and Future Direction," Tech. Rep. CR-2005-213767, NASA, 2005.

[11]Howe, M., "Noise produced by a sawtooth edge," *Journal of Acoustical Society of America*, Vol. 90, No. 1, 1991, pp. 482–487.

[12]Selig, M., Donovan, J., and Fraser, D., "Airfoils at Low Speeds," 1989.

[13]Sarradj, E., Schulze, C., and Zeibig, A., "Aspects of source separation in beamforming," *Berlin Beamforming Conference*, 2006.

[14]Brooks, T. and Humphreys, W., "Effect of Directional Array Size On The Measurement of Airframe Noise Components," AIAA Paper No. 99-1958, 1999.